

NJC

Accepted Manuscript



This is an *Accepted Manuscript*, which has been through the Royal Society of Chemistry peer review process and has been accepted for publication.

Accepted Manuscripts are published online shortly after acceptance, before technical editing, formatting and proof reading. Using this free service, authors can make their results available to the community, in citable form, before we publish the edited article. We will replace this *Accepted Manuscript* with the edited and formatted *Advance Article* as soon as it is available.

You can find more information about *Accepted Manuscripts* in the [Information for Authors](#).

Please note that technical editing may introduce minor changes to the text and/or graphics, which may alter content. The journal's standard [Terms & Conditions](#) and the [Ethical guidelines](#) still apply. In no event shall the Royal Society of Chemistry be held responsible for any errors or omissions in this *Accepted Manuscript* or any consequences arising from the use of any information it contains.

**Preparation conditions of NiS active material in high-boiling solvents
for all-solid-state lithium secondary batteries**

Keigo Aso, Akitoshi Hayashi, and Masahiro Tatsumisago

Department of Applied Chemistry, Graduate School of Engineering,
Osaka Prefecture University, 1-1 Gakuen-cho, Naka-ku, Sakai, Osaka 599-8531, Japan

Corresponding author:

Akitoshi Hayashi (Associate Professor)

Department of Applied Chemistry, Graduate School of Engineering,

Osaka Prefecture University,

1-1 Gakuen-cho, Naka-ku, Sakai, Osaka 599-8531, JAPAN

Tel.: +81-72-2549334, Fax.: +81-72-2549334

E-mail address: hayashi@chem.osakafu-u.ac.jp.

Abstract

Nickel sulfide particles were synthesized by thermal decomposition of nickel acetylacetonate in a mixed solution of 1-dodecanethiol and high-boiling solvents. Nickel sulfide was formed by thermal decomposition of nickel(II) dodecanethiolate in the high-boiling solvent, and the crystal phases of nickel sulfide were controlled by selection of the solvent. NiS was obtained in 1-octadecene as a noncoordinating solvent. On the other hand, Ni₉S₈ was prepared in oleylamine as a coordinating solvent because oleylamine molecules has a strong capping ability to nickel ions in nickel(II) dodecanethiolate, and thus the oleylamine molecules prevent the diffusion of sulfur derived from nickel(II) dodecanethiolate and free 1-dodecanethiol. All-solid-state cells were fabricated by using composite electrodes prepared by wet milling in hexane. At a current density of 1.3 mA cm⁻², the cell using a composite electrode prepared by wet milling exhibited the discharge capacity of 500 mAh g⁻¹ for 30 cycles and the better cycle performance than the cell using a composite electrode prepared by hand-grinding in a mortar.

Keyword

Nickel sulfide, thermal decomposition, capping ability, oleylamine, all-solid-state batteries

Introduction

Nanomaterials have received much attention as an active material in lithium-ion batteries [1]. In general, nano-sized active materials can decrease the diffusion length of lithium ion in the insertion/extraction process, which improves the rate performance in the lithium-ion batteries. Nanomaterials prepared by a solution process using high-boiling solvents as a surfactant have been attracting attention [2,3]. High-boiling solvents such as long-chain organic molecules are often used as reaction media. Long-chain organic molecules as a surfactant are important in this technique. Particle nucleation and growth are controlled by the long-chain organic molecules. It was reported that various metal phosphides such as MnP, Co₂P, FeP, and Ni₂P, and sulfides such as Cu₂S, ZnS, MnS, and PbS were synthesized using high-boiling solvents [4,5]. This synthesis process using high-boiling solvents makes it possible to synthesize nanoparticles with uniform size and various morphologies by varying reaction conditions. On the other hand, metal phosphides and sulfides have been applied as active materials with high capacity to lithium-ion batteries using organic liquid electrolytes or inorganic solid electrolytes [6-10].

All-solid-state lithium secondary batteries using inorganic solid electrolytes have attracted much attention for application as power sources for plug-in hybrid vehicle (PHV) and battery electric vehicles (BEV), because these batteries are extremely safe, reliable, and free from electrolyte leakage [11,12]. Much effort has been directed to develop solid electrolytes with high lithium-ion

conductivity. Sulfide-based solid electrolytes such as glasses, crystals, and glass-ceramics are promising because of high lithium-ion conductivities at room temperature. Sulfide glasses in the systems $\text{Li}_2\text{S-SiS}_2$ and $\text{Li}_2\text{S-P}_2\text{S}_5$ prepared by the melt-quenching method are known as lithium-ion conductors with high conductivities of over $10^{-4} \text{ S cm}^{-1}$ at room temperature [13-16]. Kanno *et al.* have found that the sulfide crystalline lithium superionic conductor, thio-LISICON (such as solid solutions in the system $\text{Li}_4\text{GeS}_4\text{-Li}_3\text{PS}_4$), exhibited high lithium-ion conductivities of 10^{-7} to $10^{-3} \text{ S cm}^{-1}$ at room temperature [17]. Recently, they reported the preparation of $\text{Li}_{10}\text{GeP}_2\text{S}_{12}$ solid electrolyte, which exhibited a quite high lithium-ion conductivity of over $10^{-2} \text{ S cm}^{-1}$ at room temperature [18]. On the other hand, we have reported that the crystallization of $\text{Li}_2\text{S-P}_2\text{S}_5$ glasses prepared by a mechanical milling technique improved their conductivities [19]. $\text{Li}_2\text{S-P}_2\text{S}_5$ glass-ceramic electrolytes showed a high lithium-ion conductivity of $5 \times 10^{-3} \text{ S cm}^{-1}$ at room temperature [20].

In bulk-type all-solid-state batteries, a composite positive or negative electrode consisting of three components of active materials, solid electrolytes (lithium-ion conduction path), and conductive additives (electron conduction path) is commonly used. Electrochemical reactions proceed at the solid-solid interfaces, and are affected by the states of the interfaces in the composite electrode. It is expected that the solid-solid interface in the composite electrode will increase with decreasing the particle size of monodispersed active materials. We reported that monodispersed

α -Fe₂O₃ particles of various sizes were synthesized by a solution process using a NaOH aqueous solution [21]. The all-solid-state cell with a submicron α -Fe₂O₃ electrode exhibited higher capacity than that of the cell using a micron-size α -Fe₂O₃ electrode. The dispersion state of active materials in the composite electrode as well as the morphology of active materials is very important for development of high-performance all-solid-state batteries. In addition, it is known that the particles prepared by a solution process using high-boiling solvents are dispersed in organic solvent. Simple preparation of composite electrodes with favorable solid-solid interfaces will be achieved by utilization of organic solvent (e.g. ball milling in organic solvent).

We reported that needle-like or plate-like tin sulfide (SnS) particles were synthesized by thermal decomposition of tin acetate and 1-dodecanethiol in trioctylphosphine or oleylamine, and the formation mechanism of tin sulfide was investigated by varying reaction conditions [22]. Trioctylphosphine or oleylamine are widely used as a coordinating solvent with high-boiling point. The capacity of the all-solid-state cell using needle-like SnS particles as an active material was larger than that of the cell with plate-like SnS particles. The paper also showed that needle-like SnS particles were formed by the diffusion of sulfur derived from 1-dodecanethiol into spherical Sn particles, and the aspect ratio of needle-like SnS particles was controlled by the mixing ratio of 1-dodecanethiol and trioctylphosphine. On the other hand, we reported that Ni₉S₈ and NiS nanoparticles were synthesized in high-boiling solvents, and that the composite electrodes were

prepared by hand-grinding of the mixture (nickel sulfide, sulfide solid electrolyte and conductive additive) in a mortar for application to all-solid-state cells [23]. The all-solid-state cell using NiS nanoparticles exhibited larger capacity than that of the cell using Ni₉S₈ nanorods at the current density of 0.13 mA cm⁻². This is because the theoretical capacity of NiS active material (590 mAh g⁻¹) is larger than that of Ni₉S₈ active material (550 mAh g⁻¹). Although we have investigated the effect of crystal phase of nickel sulfide on the capacity of all-solid-state batteries, both the formation mechanism of nickel sulfide and the preparation technique of the composite electrode have not been investigated in our previous paper [23]. Understanding of formation mechanism for nickel sulfide (Ni₉S₈ and NiS) may contribute to morphology-controlled synthesis of NiS active material.

In this study, the formation mechanism of nickel sulfide was investigated by changing the reaction conditions, examining intermediates, and verifying the effects of capping ability of a coordinating solvent on crystal phase of nickel sulfide. In order to increase the solid-solid interface among active material, solid electrolyte, and conductive additive, the composite electrode was prepared by ball milling of a mixture of the obtained NiS nanoparticles, the sulfide-based solid electrolytes, and carbon fibers. Organic solvent was used as a dispersant of NiS nanoparticles. Electrochemical properties of the all-solid-state cells were investigated using charge-discharge measurements.

Experimental

Nickel(II) acetylacetonate ($\text{Ni}(\text{acac})_2$; 0.385 g, 1.5×10^{-3} mol) was mixed with 1-dodecanethiol (DT; 2 ml, 8.3×10^{-3} mol) as a sulfur source in oleylamine (OAm; 10 ml, 3.0×10^{-2} mol) or 1-octadecene (ODE; 10 ml, 3.0×10^{-2} mol). OAm was used as a coordinating solvent, whereas ODE was used as a noncoordinating solvent. The mixture was heated in a flask to several temperatures (180, 240, or 280 °C), and was subsequently kept for 0, 5, or 24 hours under stirring in an Ar atmosphere. After heating, the mixture was cooled to room temperature and was subsequently washed with hexane and ethanol. The resultant particles were isolated by centrifuging the mixture and then removing the supernatants.

X-ray diffraction (XRD; UltimaIV; Rigaku) measurements were performed using Cu K α radiation to identify the crystalline phases. The thermal decomposition of the obtained intermediates was characterized by differential thermal analysis and thermogravimetry (DTA-TG; Thermo Plus 2 TG-8110; Rigaku). Fourier transform infrared (FT-IR) spectra of the obtained intermediates were measured with a FT-IR spectrophotometer (Spectrum GX; Perkin Elmer). The morphology of the obtained composite electrode was observed using scanning electron microscopy (SEM; JSM-6610A; JEOL) coupled with an energy dispersive X-ray spectrometer (EDX; JED-2300; JEOL).

Laboratory-scale solid-state cells were fabricated as follows. The 80Li₂S·20P₂S₅ (mol %) glass-ceramic solid electrolyte powder was prepared by mechanical milling of a mixture of Li₂S and P₂S₅ and subsequent heat treatment. The prepared electrolyte exhibited a wide electrochemical window and high ionic conductivity at room temperature [24]. A composite electrode of NiS, the glass-ceramic electrolyte, and vapor grown carbon fiber (VGCF) with a weight ratio of 20:30:3 was prepared by wet milling in 0.2 ml of hexane with a planetary ball mill in a dry Ar-filled glove box. A stainless steel pot (25 ml) with 400 stainless steel balls (diameter: 2 mm) was used, and the rotation speed was fixed at 210 rpm for 6 h. For comparison, the composite electrode of NiS, the glass-ceramic electrolyte, and VGCF with a weight ratio of 20:30:3 were prepared by hand-grinding of the mixture in a mortar. Two-electrode cells were fabricated using the composite electrode as a working electrode, the glass-ceramic electrolyte, and a Li-In alloy as a counter and reference electrode. The composite electrode and solid electrolyte were placed in a polycarbonate tube (10 mm diameter) and pressed together under 360 MPa at room temperature. The Li-In alloy was placed on the surface of the solid electrolyte side of the bilayer pellet. Then pressure of 120 MPa was applied to obtain a three-layered pellet. The three-layered pellet was finally sandwiched with two stainless-steel disks as current collectors. All preparation processes of the cells were conducted in a dry Ar-filled glove box. Electrochemical tests were performed under a constant current density of 1.3 mA cm⁻² at 25 °C in an Ar atmosphere using a charge-discharge measurement

device (BTS-2004, Nagano Co.).

Results and discussion

Figure 1 shows the XRD patterns of the sample prepared in OAm as a coordinating solvent at several temperatures. An intermediate was obtained by heating at 180 °C (without holding time), and then Ni_9S_8 particles were prepared at 240 °C (without holding time) and at 280 °C for 24 h. On the other hand, Figure 2 shows the XRD patterns of the sample prepared in ODE as a noncoordinating solvent at several temperatures. An intermediate was obtained by heating at 180 °C (without holding time) similar to OAm, and then NiS particles were prepared via Ni_9S_8 at 280 °C for 5 h. Nickel sulfide (Ni_9S_8 or NiS) crystals with different phase were obtained by selecting the high-boiling solvent as reaction media. We have reported that this is because OAm has a stronger capping ability than ODE [23]. Several studies on metal thiolates as the intermediate for synthesis of metal sulfides have been reported [25-27]. It is predicted that the obtained intermediate is nickel dodecanethiolate; nickel sulfides (Ni_9S_8 and NiS) are formed by thermal decomposition of nickel dodecanethiolate.

Scheme 1 shows the three synthetic routes (Routes 1, 2, and 3) for investigation of reaction mechanism of nickel sulfide. Firstly, the obtained intermediate was examined by “Route 1” shown in Scheme 1. Figure 3a shows the XRD pattern of the sample prepared by heating the intermediate

in 10 mL of ODE at 280 °C for 5 h. The obtained sample was identified as NiS. In addition, the thermal decomposition behavior of the obtained intermediate was characterized by DTA-TG measurements. Figure 3b shows the DTA-TG curves of the intermediate under N₂ flow. The sharp endothermic peak observed about 70 °C is due to melting of the intermediate, whereas the endothermic peak around 260 °C accompanied with weight loss is attributed to decomposition of the intermediate. The weight change with the decomposition is 79%, which closely corresponds to the theoretical weight change of 80% from the metal thiolate of Ni and dodecanethiol (molar ratio of 1:2) to NiS.

Figure 4a, 4b, and 4c respectively show the FT-IR spectra of 1-dodecanethiol, the intermediate prepared in OAm at 180 °C, and the intermediate prepared in ODE at 180 °C. Figure 4d, 4e, and 4f respectively show the enlarged spectra between 2650 and 2450 cm⁻¹ for 1-dodecanethiol, the intermediate prepared in OAm, and the intermediate prepared in ODE. In Figure 4a, pure 1-dodecanethiol exhibits sharp bands at 2921 cm⁻¹ and 2850 cm⁻¹ attributed to asymmetric methyl stretching vibration, and the asymmetric and symmetric methylene stretching vibration [26]. Two bands at 2921 cm⁻¹ and 2850 cm⁻¹ were clearly present in the spectra of the intermediate (Figure 4b and 4c), whereas the band at 2579 cm⁻¹ attributed to the S-H vibrations of 1-dodecanethiol (Figure 4d) was not observed in the spectra of Figure 4e and 4f. These results suggest that the obtained intermediate is nickel(II) dodecanethiolate, and nickel sulfides (Ni₉S₈ and NiS) are formed by

thermal decomposition of nickel(II) dodecanethiolate.

Additional experiments (“Route 2” and “Route 3” shown in Scheme 1) were performed in order to investigate the effects of OAm on crystal phase of nickel sulfide. As shown in Figure 2c, NiS was ordinarily obtained by heating at 280 °C for 5 h in ODE as reaction media. Figure 5 shows the XRD pattern for the sample prepared by injection of OAm (5 mL) into ODE (5 mL) at 180 °C (“Route 2”). Ni₉S₈ was obtained by injection of OAm at 180 °C. Considering that both nickel(II) dodecanethiolate and free DT act as a sulfur source in “Route 2”, the fact of the formation of Ni₉S₈ suggests that the sulfur diffusion to nickel ions in nickel(II) dodecanethiolate is prevented by OAm molecules with their strong capping ability. As another approach, Table 1 and Figure 6 respectively show the reaction conditions and XRD patterns of the samples prepared by changing the amount of OAm in the range from 10 mL to 2 mL (“Route 3”). The amount of DT (2 mL, 8.3×10^{-3} mol) was fixed, whereas the amount of OAm was changed to investigate the effect of the amount of OAm on crystal phase of nickel sulfide. ODE was used as a noncoordinating solvent, and the total volume of OAm, DT, and ODE in Table 1 was 12 mL in order to fix the concentration of nickel(II) acetylacetonate. The crystal phase of the obtained particles was changed from Ni₉S₈ to NiS by decreasing the amount of OAm against the fixed amount of DT. This is because the fraction of free DT that is not related to the formation of nickel(II) dodecanethiolate relatively increased compared to the fraction of OAm. The results of these additional experiments (“Route

2” and “Route 3”) suggest that the excessive amount of OAm molecules has a strong capping ability to nickel ions in nickel(II) dodecanethiolate, and thus the OAm molecules prevent the diffusion of sulfur derived from nickel(II) dodecanethiolate and free DT.

The contact area among active materials, solid electrolytes, and conductive additives as well as the morphology of active materials are important for development of high-performance all-solid-state batteries. We reported that a composite electrode using NiS for all-solid-state batteries was prepared by hand-grinding of a mixture of NiS nanoparticles, the 80Li₂S·20P₂S₅ solid electrolyte, and VGCF in a mortar [23]. XRD pattern of the composite electrode prepared by hand-grinding of the mixture is shown in Figure S1, and the NiS particles which were synthesized in ODE at 280 °C for 5 h (Figure 2c) were used as an active material. In this study, a composite electrode was prepared by wet milling in hexane as a dispersant of the NiS particles in order to increase the contact area among the three components. Figure 7a shows the SEM image and EDX mapping image for Ni element of the surface of the pelletized composite electrode prepared by wet milling in hexane, whereas Figure 7b shows those of the surface of the pelletized composite electrode prepared by hand-grinding of NiS, the solid electrolyte, and VGCF in a mortar. The result of EDX analysis in Figure 7a shows that NiS nanoparticles were dispersed uniformly on the surfaces of solid electrolyte in the composite electrode. On the other hand, from the EDX mapping image in Figure 7b, NiS nanoparticles were aggregated in the composite electrode (bright

part, NiS nanoparticles; dark part, solid electrolytes).

In our previous paper [23], the all-solid-state cell using NiS nanoparticles were performed under a low current density of 0.13 mA cm^{-2} . In this paper, in order to investigate effects on the electrochemical performance of the dispersion state of NiS active materials in the composite electrodes, the cells were performed under higher current density of 1.3 mA cm^{-2} . Figure 8a shows the charge-discharge curves of the all-solid-state cell using the composite electrode prepared by wet milling in hexane at the 10th, 20th, and 30th cycles under a current density of 1.3 mA cm^{-2} . For comparison, the charge-discharge curves of the all-solid-state cell using the composite electrode prepared by hand-grinding in a mortar under the current density of 1.3 mA cm^{-2} are also shown in Figure 8a. Li-In alloy was used as a counter electrode because Li-In alloy exhibits a stable potential plateau at $0.62 \text{ V vs. Li}^+/\text{Li}$, as observed in all-solid-state cells with sulfide electrolytes. In Figure 8a, the left-side ordinate axis shows the electrode potential vs. Li-In, while the right-side ordinate axis shows the electrode potential vs. Li, which is calculated based on the potential difference between Li-In and Li electrodes (0.62 V). The obtained capacity was normalized by the weight of NiS in the composite electrode. The all-solid-state cell using the composite electrode prepared by wet milling in hexane retained a discharge capacity of 500 mAh g^{-1} and a charge-discharge efficiency of approximately 100% after 30 cycles in the voltages of $1.0\text{-}4.0 \text{ V}$ (vs. Li) under the current density of 1.3 mA cm^{-2} at $25 \text{ }^\circ\text{C}$. The capacity of 500 mAh g^{-1} corresponds

to that of 190 mAh g⁻¹ normalized by the weight of the whole composite electrode. Figure 8b shows the cycle performance of the all-solid-state cells using two different composite electrodes. The cell using the composite electrode prepared by wet milling in hexane exhibited better cycle performance than the cell using the electrode prepared by hand-grinding in a mortar. This result suggests that cell performance was affected by the dispersion state of active materials in the composite electrode, and the formation of intimate solid-solid interfaces gives favorable lithium-ion and electron conduction paths to NiS nanoparticles in the composite electrode prepared by wet milling in hexane. The utilization of wet milling in organic solvent for preparation of composite electrode was effective for developing the electrochemical performance of all-solid-state batteries.

Conclusions

Nickel sulfide particles were synthesized from nickel(II) acetylacetonate and DT in OAm or ODE. Ni₉S₈ was obtained by using OAm as a coordinating solvent, whereas NiS was prepared by using ODE as a noncoordinating solvent. Both Ni₉S₈ and NiS were formed via thermal decomposition of nickel(II) dodecanethiolate. Nickel sulfide crystals with different phase were obtained by selecting the solvent (OAm or ODE) as reaction media, because the excessive amount of OAm molecules has a strong capping ability to nickel ions in nickel(II) dodecanethiolate, and the OAm molecules prevent the diffusion of sulfur derived from nickel(II) dodecanethiolate and free

DT. A composite electrode was prepared by wet milling in hexane as a dispersant of NiS nanoparticles in order to increase the contact area among the three constituents (NiS nanoparticle, the 80Li₂S·20P₂S₅ solid electrolyte, and VGCF). At 1.3 mA cm⁻² at 25 °C, the all-solid-state cell using the composite electrode prepared by wet milling in hexane showed the discharge capacity of 500 mAh g⁻¹ after 30 cycles, and exhibited better cycle performance than the cell using the composite electrode prepared by hand-grinding in a mortar.

Acknowledgements

This research was financially supported by the Japan Science and Technology Agency (JST), Core Research for Evolutional Science and Technology (CREST) project. K.A. is thankful for a Grant-in-Aid received as a Japan Society for the Promotion of Science (JSPS) Fellow.

References

- [1] P.G. Bruce, B. Scrosati and J.-M. Tarascon, *Angew. Chem. Int. Ed.*, 2008, 47, 2930-2946.
- [2] J. Park, J. Joo, G.K. Soon, Y. Jang and T. Hyeon, *Angew. Chem. Int. Ed.*, 2007, 46, 4630-4660.
- [3] S.G. Kwon and T. Hyeon, *Small*, 2011, 7, 2685-2702.

- [4] J. Park, B. Koo, K.Y. Yoon, Y. Hwang, M. Kang, J.-G. Park and T. Hyeon, *J. Am. Chem. Soc.*, 2005, 127, 8433-8440.
- [5] S.-H. Choi, K. An, E.-G. Kim, J.H. Yu, J.H. Kim and T. Hyeon, *Adv. Funct. Mater.*, 2009, 19, 1645-1649.
- [6] J. Cabana, L. Monconduit, D. Larcher and M.R. Palacín, *Adv. Mater.*, 2010, 22, E170-E192.
- [7] A. Hayashi, A. Inoue and M. Tatsumisago, *J. Power Sources*, 2009, 189, 669-671.
- [8] K. Takada, Y. Kitami, T. Inada, A. Kajiyama, M. Kouguchi, S. Kondo, M. Watanabe and M. Tabuchi, *J. Electrochem. Soc.*, 2001, 148, A1085-A1090.
- [9] B.-C. Kim, K. Takada, N. Ohta, Y. Seino, L. Zhang, H. Wada and T. Sasaki, *Solid State Ionics*, 2005, 176, 2383-2387.
- [10] B.T. Hang, T. Ohnishi, M. Osada, X. Xu, K. Takada and T. Sasaki, *J. Power Sources*, 2010, 195, 3323-3327.
- [11] J.W. Fergus, *J. Power Sources*, 2010, 195, 4554-4569.
- [12] K. Takada, *Acta Mater.*, 2013, 61, 759-770.
- [13] R. Mercier, J.-P. Malugani, B. Fahys and G. Robert, *Solid State Ionics*, 1981, 5, 663-666.
- [14] A. Pradel and M. Ribes, *Solid State Ionics*, 1986, 18/19, 351-355.
- [15] J. H. Kennedy, *Mater. Chem. Phys.*, 1989, 23, 29-50.
- [16] T. Minami, A. Hayashi and M. Tatsumisago, *Solid State Ionics*, 2000, 136-137, 1015-1023.

- [17] R. Kanno and M. Murayama, *J. Electrochem. Soc.*, 2001, 148, A742-A746.
- [18] N. Kamaya, K. Homma, Y. Yamakawa, M. Hirayama, R. Kanno, M. Yonemura, T. Kamiyama, Y. Kato, S. Hama, K. Kawamoto and A. Mitsui, *Nat. Mater.*, 2011, 10, 682-686.
- [19] F. Mizuno, A. Hayashi, K. Tadanaga and M. Tatsumisago, *Adv. Mater.*, 2005, 17, 918-921.
- [20] A. Hayashi, K. Minami, S. Ujiie and M. Tatsumisago, *J. Non-Cryst. Solids*, 2010, 356, 2670-2673.
- [21] H. Kitaura, K. Takahashi, F. Mizuno, A. Hayashi, K. Tadanaga and M. Tatsumisago, *J. Electrochem. Soc.*, 2007, 154, A725-A729.
- [22] K. Aso, A. Hayashi and M. Tatsumisago, *Cryst. Growth Des.*, 2011, 11, 3900-3904.
- [23] K. Aso, H. Kitaura, A. Hayashi and M. Tatsumisago, *J. Mater. Chem.*, 2011, 21, 2987-2990.
- [24] A. Hayashi, S. Hama, T. Minami and M. Tatsumisago, *Electrochem. Commun.*, 2003, 5, 111-114.
- [25] Z. Yang, A.B. Smetana, C.M. Sorensen and K.J. Klabunde, *Inorg. Chem.*, 2007, **46**, 2427-2431.
- [26] Y. Wang, Y. Hu, Q. Zhang, J. Ge, Z. Lu, Y. Hou and Y. Yin, *Inorg. Chem.*, 2010, **49**, 6601-6608.
- [27] Z. Zhuang, X. Lu, Q. Peng and Y. Li, *Chem. Eur. J.*, 2011, **17**, 10445-10452.

Figure captions

Table 1. Reaction conditions for the samples prepared by changing the amount of oleylamine (OAm). The amount of 1-dodecanethiol (DT) was fixed. Octadecene (ODE) was used as a noncoordinating solvent in order to fix the concentration of nickel(II) acetylacetonate.

Scheme 1. Synthetic routes for investigation of reaction mechanism of nickel sulfide.

Figure 1 XRD patterns of the samples prepared by heating at (a) 180 °C, (b) 240 °C, (c) 280 °C for 5 h, and (d) 280 °C for 24 h in oleylamine (OAm).

Figure 2 XRD patterns of the samples prepared by heating at (a) 180 °C, (b) 240 °C, and (c) 280 °C for 5 h in octadecene (ODE).

Figure 3 (a) XRD pattern of the sample prepared by heating the intermediate in ODE at 280 °C for 5 h (“Route 1” shown in Scheme 1). (b) DTA-TG curves of the intermediate under N₂ flow.

Figure 4 (a-c) FT-IR spectra of (a) 1-dodecanethiol and (b,c) intermediate prepared by heating at 180 °C in (b) OAm or (c) ODE. (d-f) show the enlarged spectra between 2650 and 2450 cm⁻¹ for

the (a-c) samples.

Figure 5 XRD pattern of the sample prepared by injection of OAm at 180 °C (“Route 2” shown in Scheme 1).

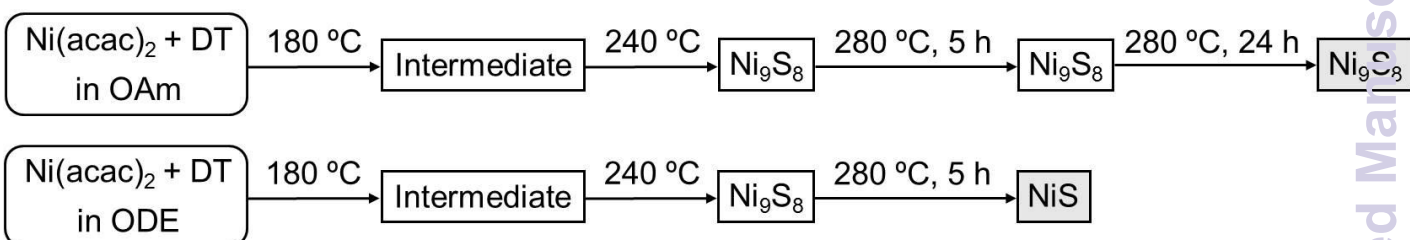
Figure 6 XRD patterns of the samples prepared by changing the amount of OAm (“Route 3” shown in Scheme 1).

Figure 7 SEM images and EDX mapping images for Ni element of (a) the composite electrode prepared by wet milling of NiS, solid electrolyte, and VGCF in hexane, and (b) the composite electrode prepared by hand-grinding of NiS, solid electrolyte, and VGCF in a mortar.

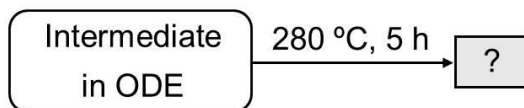
Figure 8 (a) Charge-discharge curves and (b) cycle performance of the all-solid-state cells with the composite electrode prepared by wet milling in hexane and by hand-grinding in a mortar under the current density of 1.3 mA cm⁻².

Table 1. Reaction conditions for the samples prepared by changing the amount of oleylamine (OAm). The amount of 1-dodecanethiol (DT) was fixed. Octadecene (ODE) was used as a noncoordinating solvent in order to fix the concentration of nickel(II) acetylacetonate.

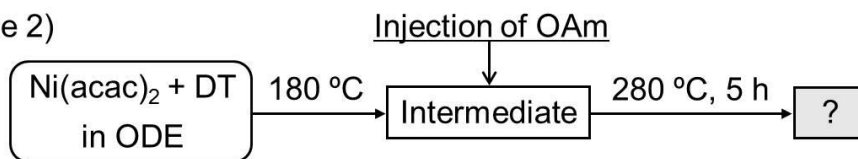
Sample	Amount of OAm	Amount of DT	OAm/DT (molar ratio)	Amount of ODE
(a)	10 mL (3.0×10^{-2} mol)	2 mL (8.3×10^{-3} mol)	3.6	—
(b)	5 mL (1.5×10^{-2} mol)	2 mL (8.3×10^{-3} mol)	1.8	5 mL (1.5×10^{-2} mol)
(c)	2 mL (6.0×10^{-3} mol)	2 mL (8.3×10^{-3} mol)	0.72	8 mL (2.4×10^{-2} mol)



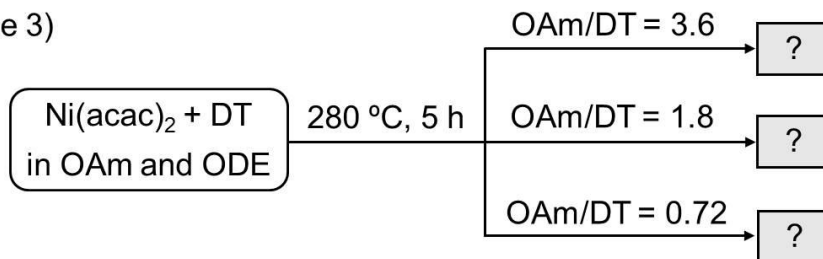
(Route 1)



(Route 2)



(Route 3)



Scheme 1. Synthetic routes for investigation of reaction mechanism of nickel sulfide.

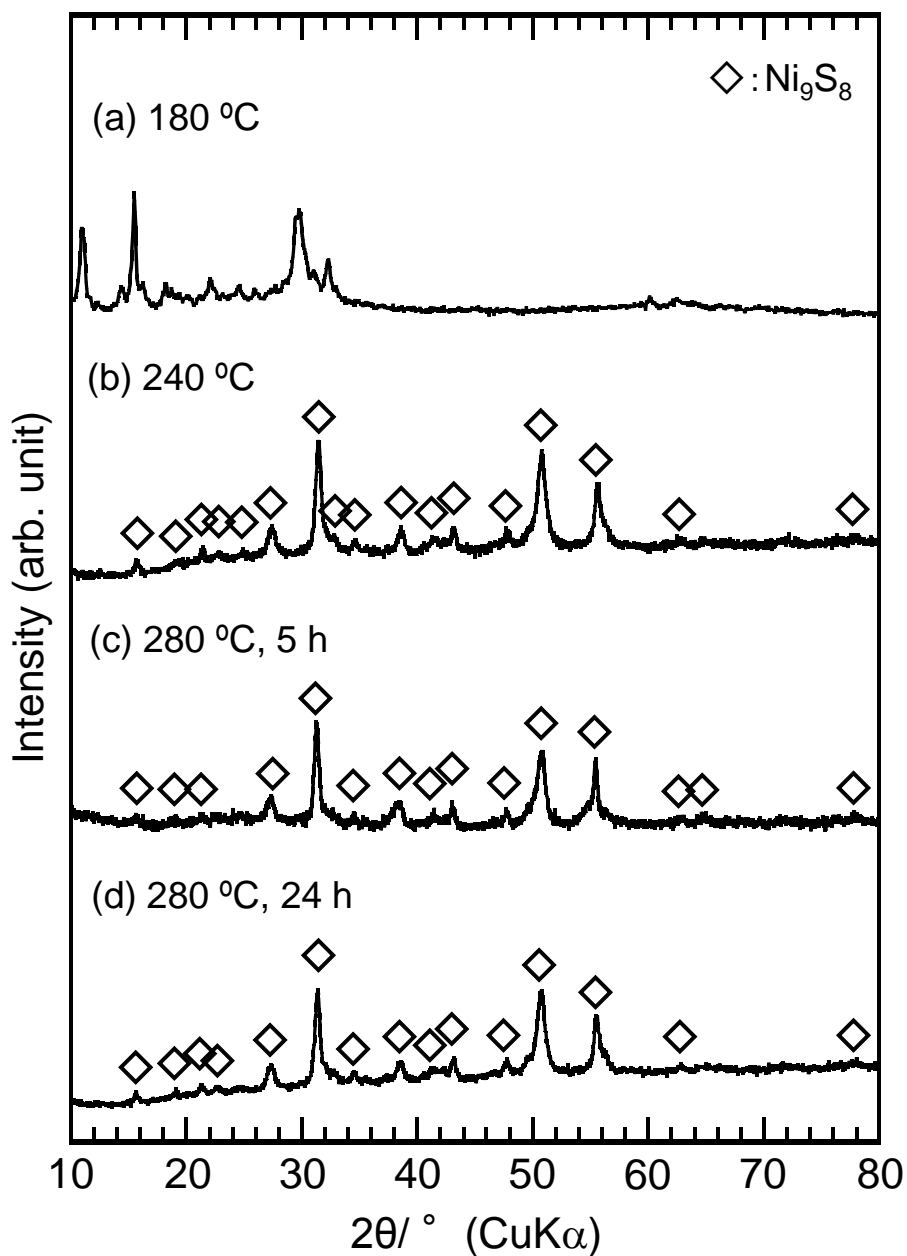


Fig. 1 XRD patterns of the samples prepared by heating at (a) 180 °C, (b) 240 °C, (c) 280 °C for 5 h, and (d) 280 °C for 24 h in oleylamine (OAm).

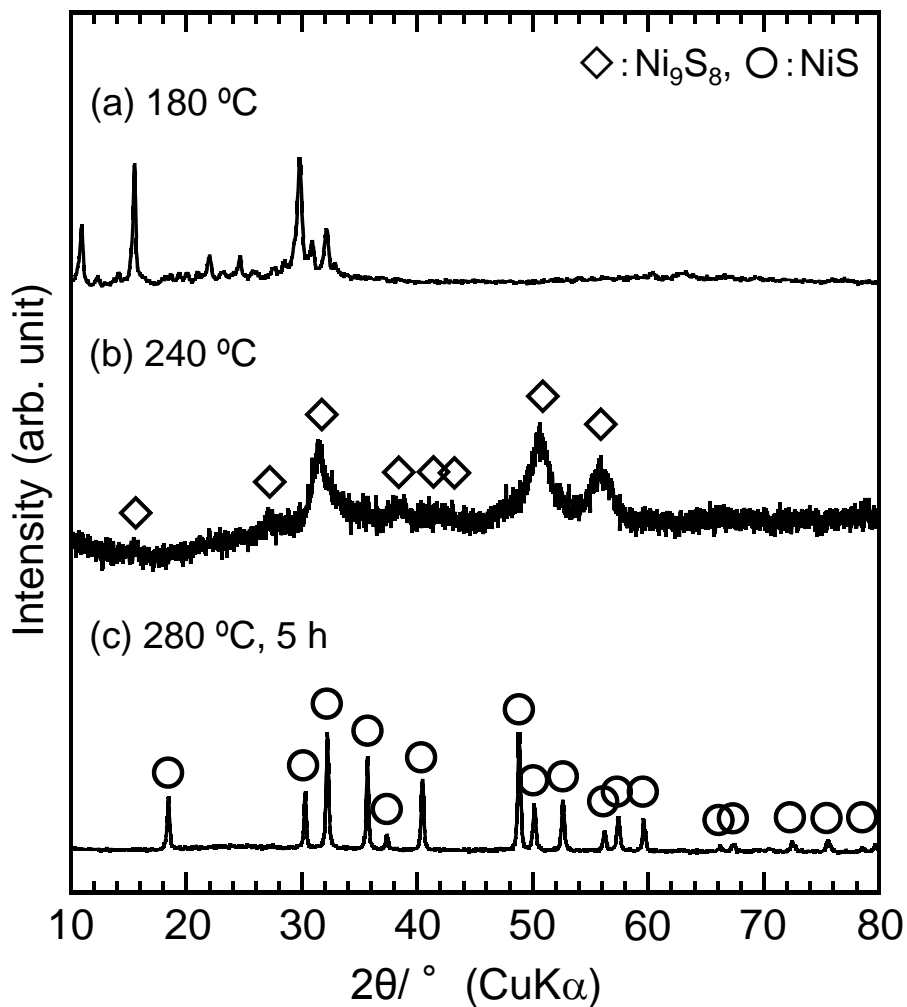


Fig. 2 XRD patterns of the samples prepared by heating at (a) 180 °C, (b) 240 °C, and (c) 280 °C for 5 h in octadecene (ODE).

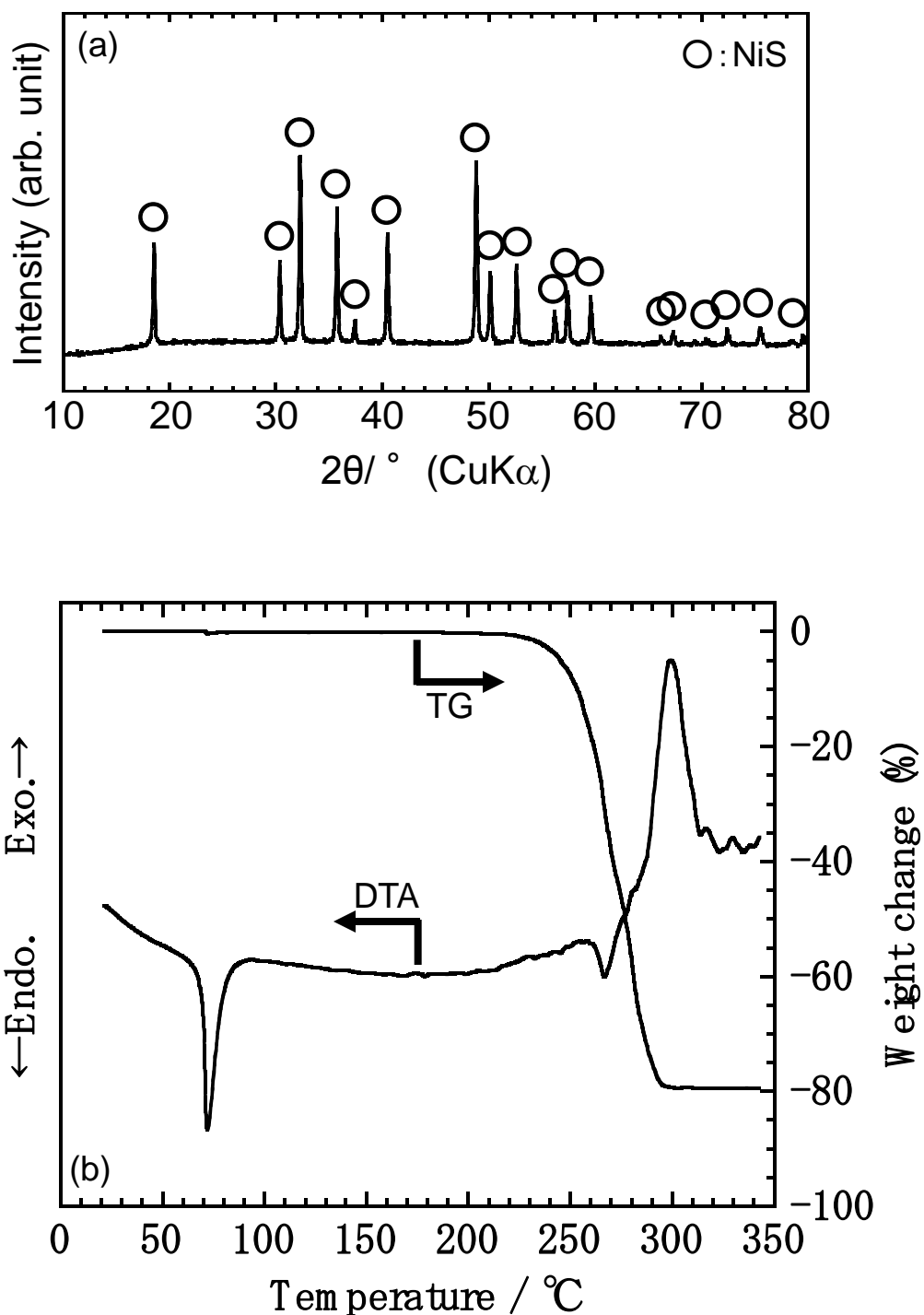


Fig. 3 (a) XRD pattern of the sample prepared by heating the intermediate in ODE at 280 °C for 5 h (“Route 1” shown in Scheme 1). (b) DTA-TG curves of the intermediate under N₂ flow.

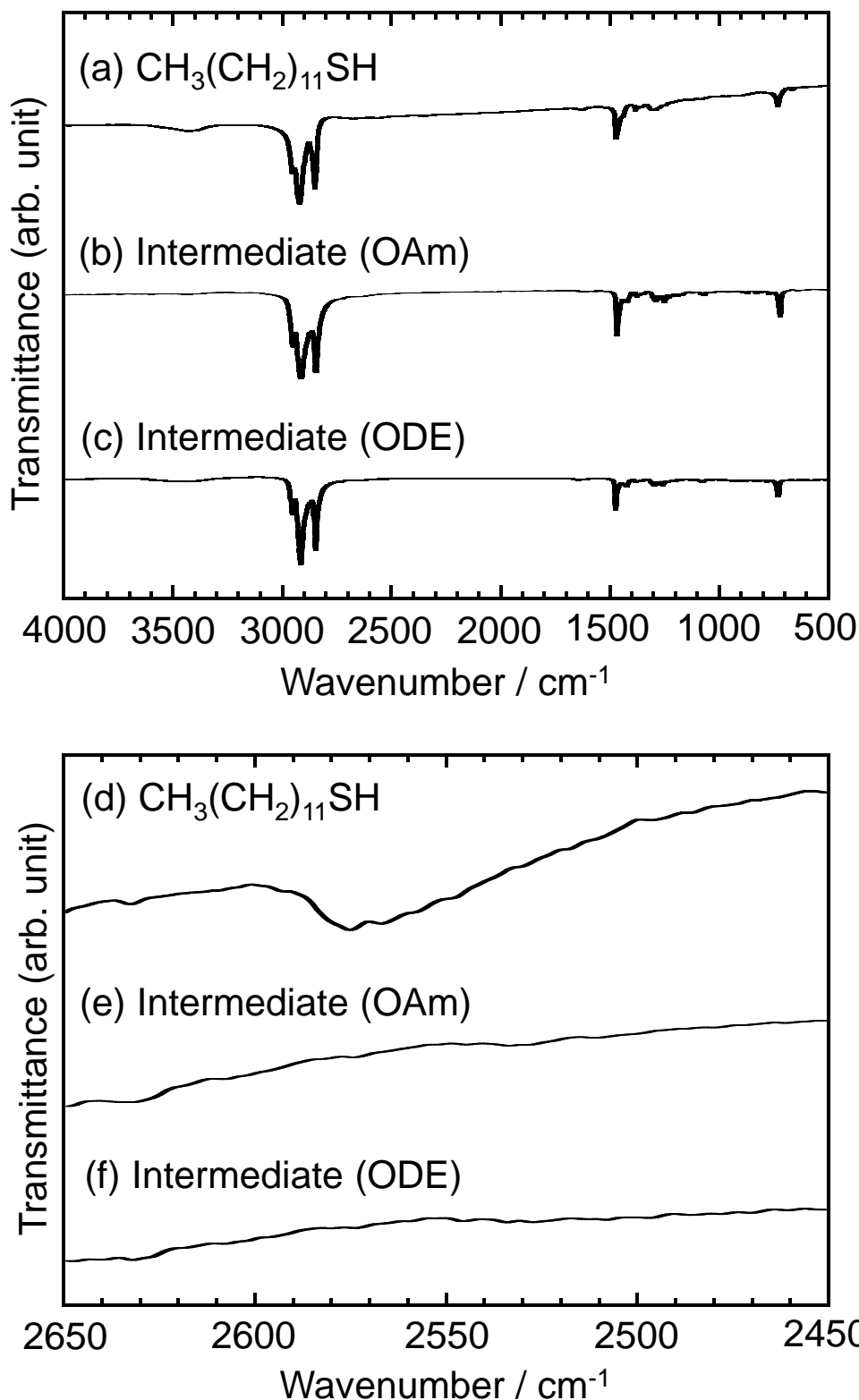


Fig. 4 (a-c) FT-IR spectra of (a) 1-dodecanethiol and (b,c) intermediate prepared by heating at 180 °C in (b) OAm or (c) ODE. (d-f) show the enlarged spectra between 2650 and 2450 cm⁻¹ for the (a-c) samples.

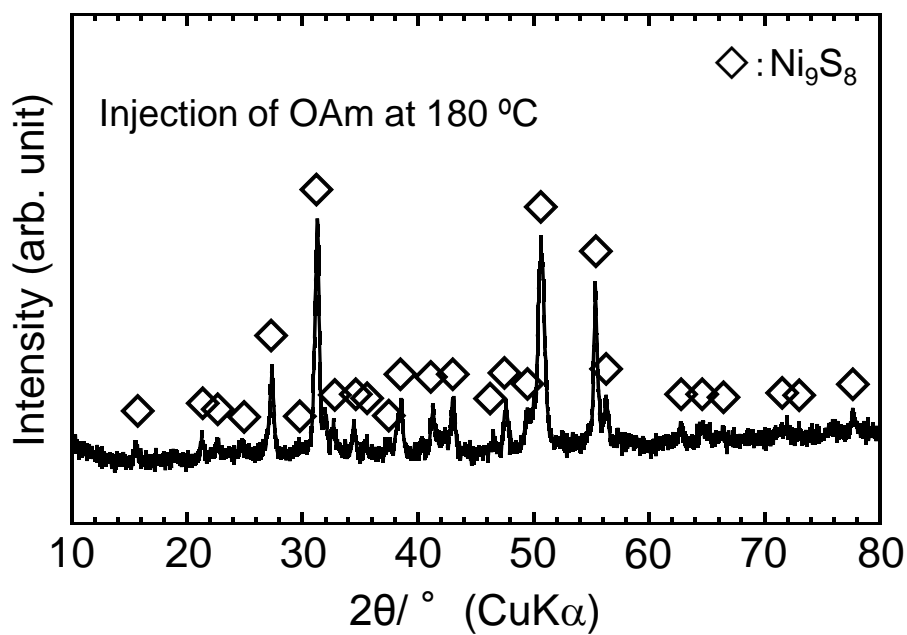


Fig. 5 XRD pattern of the sample prepared by injection of OAm at 180 °C (“Route 2” shown in Scheme 1).

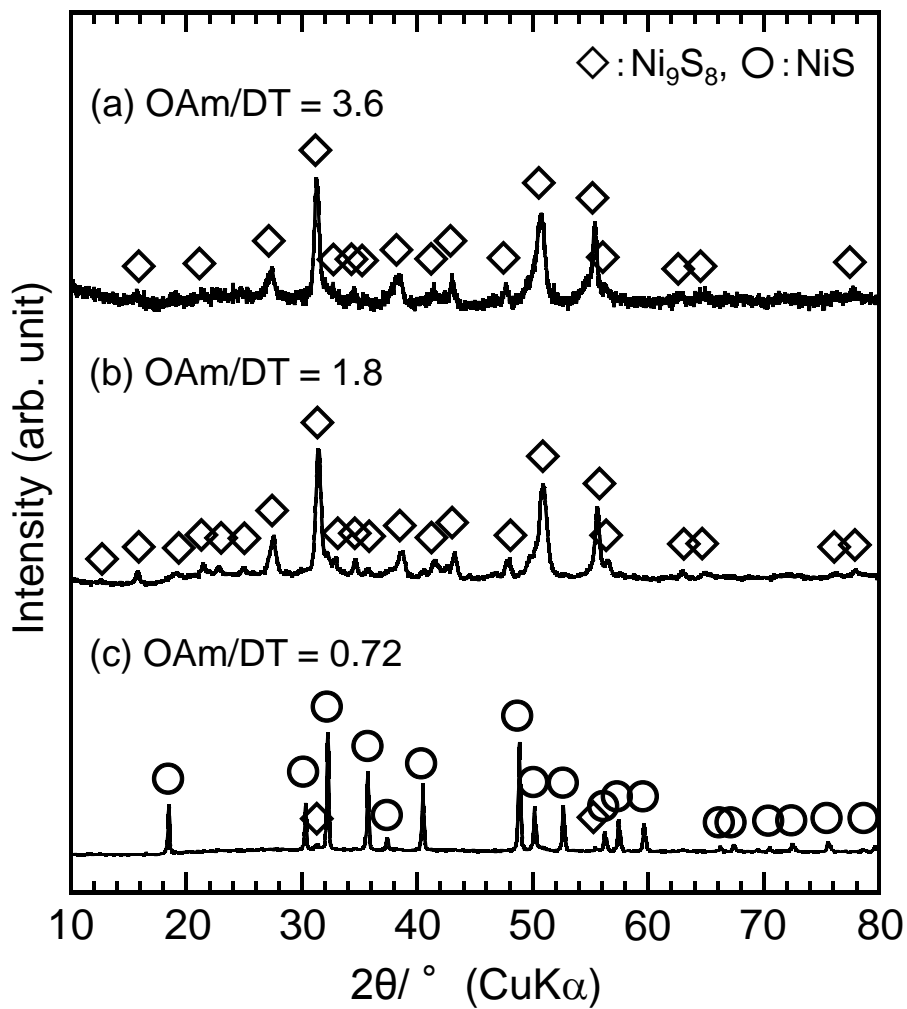
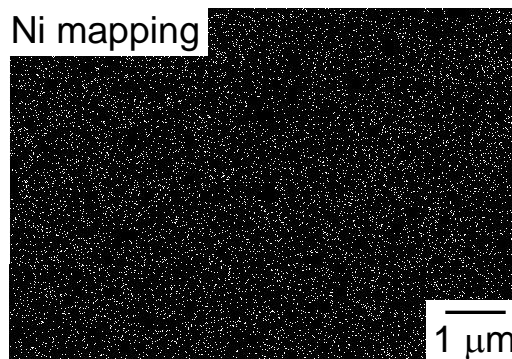
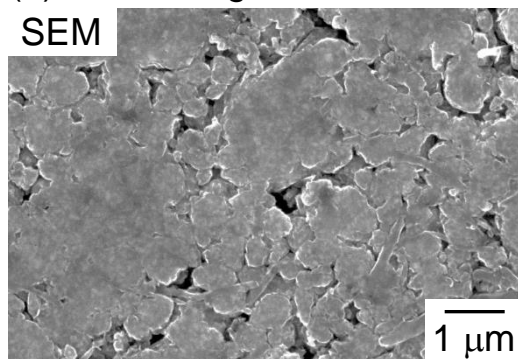


Fig. 6 XRD patterns of the samples prepared by changing the amount of OAm ("Route 3" shown in Scheme 1).

(a) Wet milling



(b) Hand-grinding in a mortar

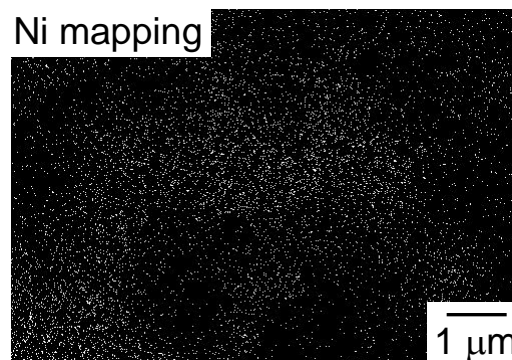
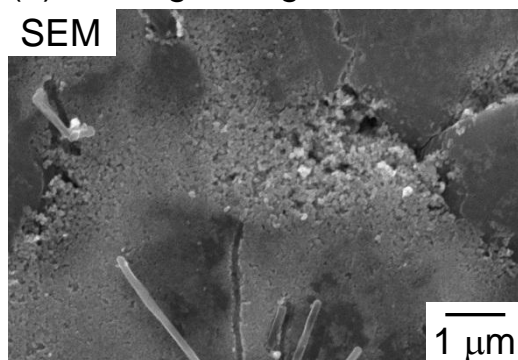


Fig. 7 SEM images and EDX mapping images for Ni element of (a) the composite electrode prepared by wet milling of NiS, solid electrolyte, and VGCF in hexane, and (b) the composite electrode prepared by hand-grinding of NiS, solid electrolyte, and VGCF in a mortar.

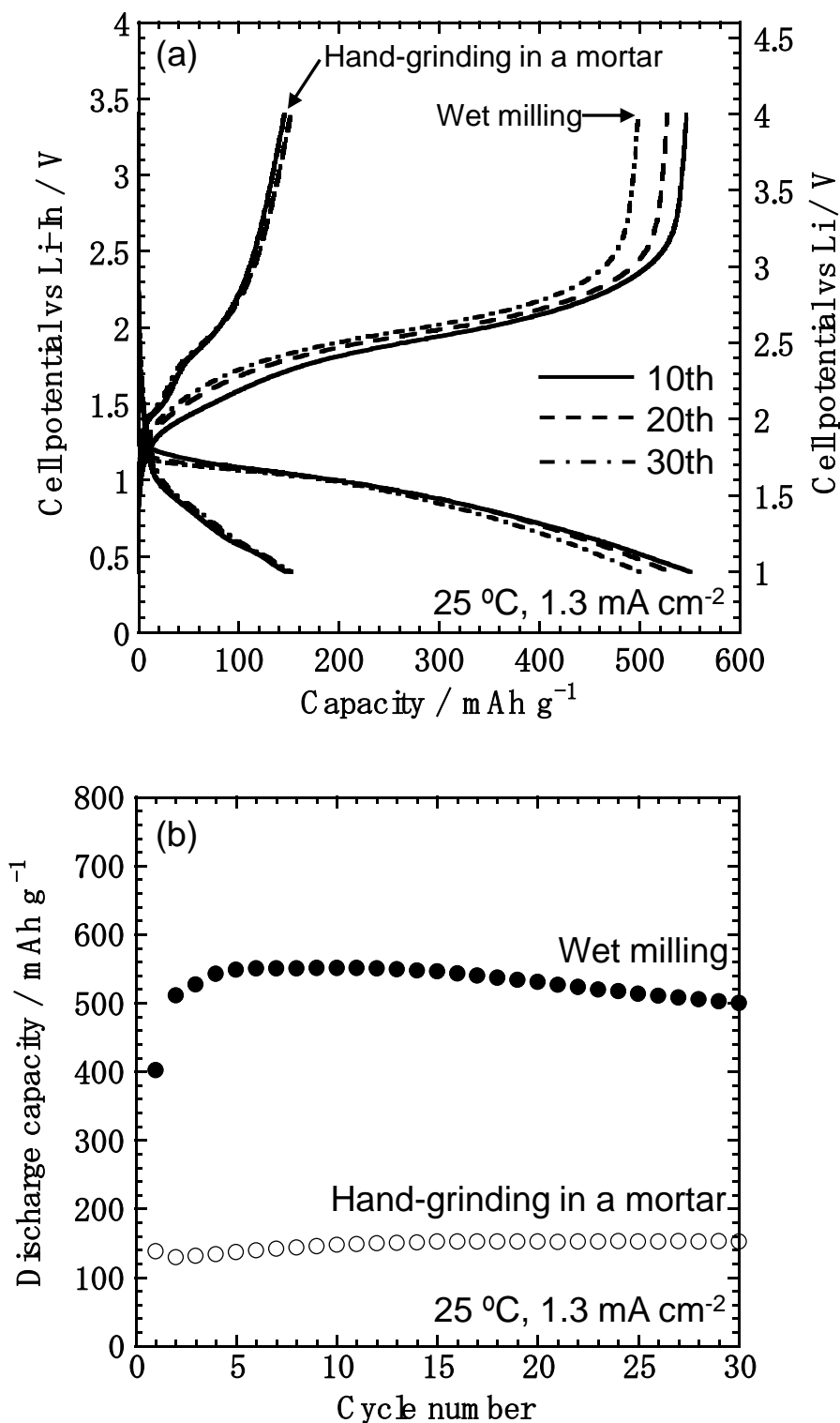
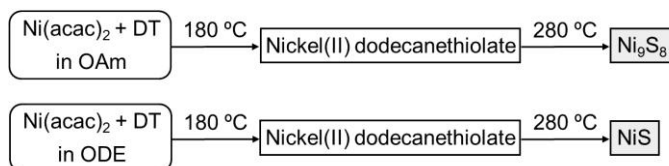


Fig. 8 (a) Charge-discharge curves and (b) cycle performance of the all-solid-state cells with the composite electrode prepared by wet milling in hexane and by hand-grinding in a mortar under the current density of 1.3 mA cm⁻².

Graphical Abstract



Formation mechanism of nickel sulfide was investigated by changing reaction conditions, examining intermediates, and verifying the effects of capping ability of a coordinating solvent on crystal phases of nickel sulfide. (30 words)